

QUASAR ABSORPTION STUDIES

NASA Grant No. NAG5-13160

Final Report

For Period 1 April 2003 through 31 March 2004

**Principal Investigator
Martin Elvis**

July 2004

Prepared for:

**National Aeronautics and Space Administration
Goddard Space Flight Center
Greenbelt, MD 20771**

**Smithsonian Institution
Astrophysical Observatory
Cambridge, Massachusetts 02138**

**The Smithsonian Astrophysical Observatory
is a member of the
Harvard-Smithsonian Center for Astrophysics**

**The NASA Technical Officer for this Grant is Richard Mushotzky, Code 662, Goddard
Space Flight Center, Greenbelt, MD 20771**

Final report Chandra award NAG5-13160, M. Elvis

Grant NAG5-13160 includes XMM-Newton proposal 14767 "Quasar absorption studies", PI. F. Fiore, SAO Co.Is: M. Elvis, A. Siemiginowska, F. Nicastro.

The aim of the proposal is to investigate the absorption properties of a sample of intermediate redshift quasars. The main goals of the project are:

- measure the redshift and the column density of the X-ray absorbers;
- test the correlation between absorption and redshift suggested by ROSAT (Fiore et al. 1998, ApJ, 492, 79, Elvis et al. 1998, ApJ, 492, 91) and ASCA (Reeves & Turner 2000, MNRAS, 316, 234) data;
- constrain the absorber ionization status and metallicity;
- constrain the absorber dust content and composition through the comparison between the amount of X-ray absorption and optical dust extinction.

Unanticipated low energy cut-offs were discovered in ROSAT spectra of quasars (Elvis et al. 1994, ApJ, 422, 60) and confirmed by ASCA (see e.g. Reeves & Turner 2000, MNRAS, 316, 234), BeppoSAX and Chandra. In most cases it was not possible to constrain adequately the redshift of the absorber from the X-ray data alone. Two possibilities remain open: **a) absorption at the quasar redshift; and b) intervening absorption.** The evidences in favour of intrinsic absorption are all indirect. Sensitive XMM observations can discriminate between these different scenarios. If the absorption is at the quasar redshift we can study whether the quasar environment evolves with the Cosmic time. A tantalizing indication that this may be the case comes from the Elvis et al. (1998, ApJ, 492, 91) finding that while $z=0.1-1$ X-ray absorbed quasars are often dusty (their optical spectrum is usually very red), the higher- z X-ray absorbed ROSAT quasars have low dust content and have associated, highly ionized optical-UV absorbers. Further pieces of evidence for an evolution of the quasar environment come from the discovery of many high- z quasars which are possibly highly obscured in X-rays but not in the optical band in BeppoSAX, ASCA, Chandra and XMM hard X-ray surveys.

In the framework of the proposal two quasars have been observed by XMM-Newton: PKS1334-127 and IRAS09104+4109.

PKS1334-127 is a compact, flat spectrum, radio loud quasar at $z=0.539$. It has a "blue" optical continuum but X-ray absorption at the level of $0.5-1 \times 10^{21} \text{ cm}^{-2}$ has been reported based on a ROSAT PSPC observation (Fiore et al. 1998, ApJ, 492, 79).

IRAS09104+4109 is a Hyperluminous Infrared Galaxy of luminosity $> 10^{12} L_{\odot}$, residing in the core of a rich cluster of galaxies at 0.442. The cluster X-ray emission can hardly be separated from AGN emission below 10 keV with the ASCA and BeppoSAX PSF. However, BeppoSAX detected in this quasar emission above 10 keV, likely due to AGN emission emerging from an absorbing screen of column density $> 10^{24} \text{ cm}^{-2}$ (Franceschini et al. 2000, A&A, 353, 910). Thanks to the high sensitivity up to 10-12 keV and its sharp PSF XMM can easily confirm this suggestion through the detection of a cold (6.4 keV) line and by separating the AGN nuclear emission from the cluster emission.

Observations and data analysis

The observations were performed with the European Photon Imaging Camera (EPIC), composed by one pn back-illuminated CCD array (Strüder et al. 2001, A&A, 365, L18) and

by two mos front-illuminated CCD arrays (Turner et al. 2001, A&A, 365, L27), named mos1 and mos2 respectively.

Unwanted periods of high particle background were rejects, leading to a net pn exposure time of 9200 sec (IRAS09104+4109) and 10900 sec (PKS1334-127). The exposure time in each mos is typically ~ 3000 sec longer than the pn exposure.

Single events are used for the pn and single+double for the mos cameras.

The source counts in each camera have been obtained using the events files, in the energy range 0.5-10 keV for the pn and 0.3-10 keV for the mos. The counts of the two mos cameras were combined. The counts of each source have been extracted in a circular region with a radius of 35 arcsec for PKS1334-127 and 18 arcsec for IRAS09104+4109. For the latter sources we kept the extraction radius as small as possible to lessen the contamination from the cluster of galaxy.

For PKS1334-127 background spectra have been extracted from nearby source free regions. For IRAS09104+4109 we decided not to subtract any background. The resulting spectrum is therefore the sum of the AGN and cluster emission.

The ancillary response files were generated for each source by means of the tool ARFGEN (SAS 5.4.1¹), The response matrix file, updated for all the observation modes to January 29, 2003 and available at the XMM-Newton archive², was adopted.

The spectral counts were accumulated in energy bins with 20 counts each, from 0.3 keV to 10 keV in the mos, and from 0.5 to 10 keV in the pn. They were then fitted, using XSPEC (version 11.2.0) using the χ^2 statistic.

Results

PKS1334-127

Fig. 1a) shows the pn+mos count spectra of PKS1334-127 along with the residuals after subtracting the best fit power law + Galactic absorption model. Significant negative residuals are visible below 0.5 keV, together with positive residuals around 1 keV, both indicating the presence of absorption. We have then fitted the spectra adding an absorption component at the redshift of the quasar. Best fits are in Table 1. Fig. 1b) shows the 67%, 90% and 99% $\Gamma-N_H \chi^2$ contours. We conclude that significant absorption, similar to that detected by the ROSAT PSPC, is present in the spectrum of PKS1334-127.

IRAS09104+4109

Fig. 2 shows the 0.5-2 keV and 7-11 keV images of the field centred on IRAS09104+4109. Note as the cluster extended emission completely dominates the soft X-ray emission, while the AGN stands out in the hard band image.

The spectrum of IRAS09104+4109 is rather complex. We have first fitted it with a model including the thermal emission from the cluster of galaxy (the XSPEC MEKAL model)

Fig. 3a) shows the pn+mos count spectra of IRAS09104+4109 along with the best fit thermal model. Note the large excess at high energies and the residual at ~ 4.4 keV (6.4 keV

¹http://xmm.vilspa.esa.es/external/xmm_sw_cal/sas.frame.shtml

²<ftp://xmm.vilspa.esa.es/pub/ccf/constituents/extras/responses/>

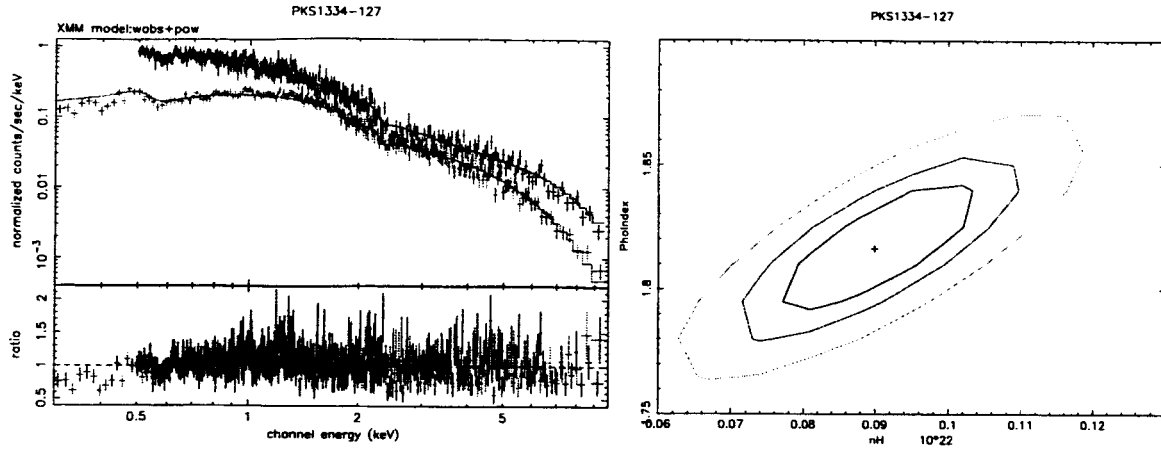


Figure 1: a), left: the PKS1334-127 pn+mos count spectra and best fit power law + Galactict absorption model, along with the residuals after subtracting the best fit model (lower panel). b)

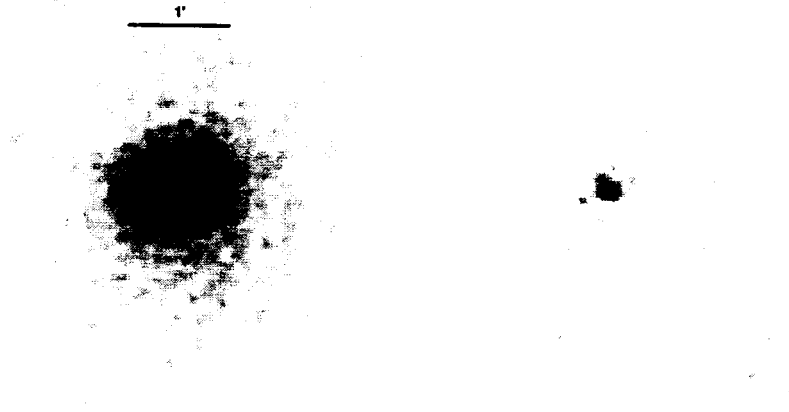


Figure 2: EPIC pn images of the IRAS09104+4109 field in the 0.5-2 keV (left) and 7-11 keV (right) bands)

Table 1: **Spectral fits**

PKS1334-127					
model	χ^2 (dof)	$N_H z = z_e m$	α		
PL.	601.7 (558)	0.	1.68 ± 0.02		
PL+abs ($z=0.539$)	497.4 (557)	0.9 ± 0.2	1.82 ± 0.02		
IRAS09104+4109					
model	χ^2 (dof)	T (keV)	Abund.	AGN L(0.7-10keV)	Fe E.W. eV
Th.	460.2 (415)	5.6 ± 0.1	0.5		
Th.+refl.	393.75 (412)	3.9 ± 0.2	0.5	$10^{44} \text{ erg s}^{-1}$	70
$N_H 10^{23} \text{cm}^{-2}$					
Th.+PL+abs.	383.4 (411)	4.2 ± 0.2	50^{+30}_{-20}	2.2×10^{45}	90

rest frame). Both residual clearly indicate a strong AGN component. The AGN component has been parameterized in two different ways. First, we have assumed a pure reflection component (XSPEC PEXRAW+ZGAUSS models). Best fits are again in Table 1. Fig. 3b) shows the best fit thermal + pure reflection model. No primary radiation is visible in the XMM spectrum. The 0.7-10 keV luminosity of the reflection component is $\sim 10^{44} \text{ erg s}^{-1}$, similar to that reported by Iwasawa et al. (2001, MNRAS, 321, L15). Assuming an albedo of ~ 0.05 the luminosity of the primary source can be as high as $2 \times 10^{45} \text{ erg s}^{-1}$. Second, we have assumed a highly absorbed power law plus an iron line. In this case, the high energy excess in the residual of Fig. 3 is explained in terms of direct emission piercing through a thick absorption screen. The best fit column density is 5×10^{23} , lower than that reported by Franceschini et al (1999), which however fit the full 1-70 keV band. The next step will be to fit simultaneously the XMM data and the BeppoSAX PDS data, to extend the band to 70 keV. The luminosity of the AGN component (deobscured) is $2.2 \times 10^{45} \text{ erg s}^{-1}$.

A paper presenting the results briefly illustrated in this report is in preparation.

Best Regards,

Fabrizio Fiore, Simonetta Puccetti, Martin Elvis

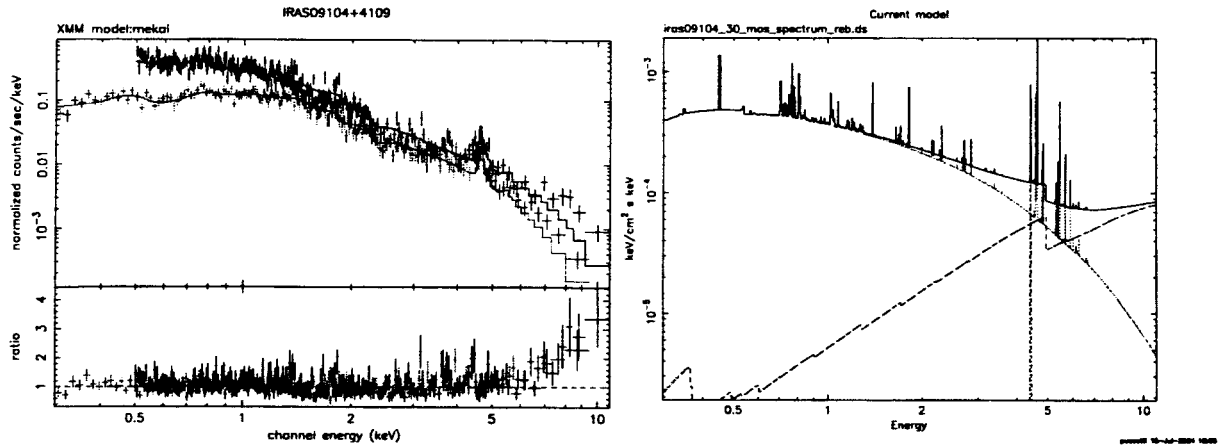


Figure 3: a), left: the IRAS09104+4109 pn+mos count spectra and best fit thermal (MEKAL) model, along with the residuals after subtracting the best fit model (lower panel). b), right panel: the best fit thermal + pure reflection model.